NOTES AND CORRESPONDENCE

A Kinematic Model of Wind-Driven Meridional Heat Transport

BARRY A. KLINGER

Oceanographic Center, Nova Southeastern University, Dania, Florida

9 May 1994 and 22 May 1995

ABSTRACT

A kinematic model of flow in the subtropical gyre is used to estimate the upper-ocean temperature distribution and heat transport that is forced by the wind-driven circulation. The temperature is idealized as a passive tracer forced by a zonally constant Haney condition and advected by a barotropic gyre. The simplicity of the model allows for analytical solutions, which are in fairly good quantitative agreement with the results obtained by Wang et al. using a numerical model. In particular, the maximum heat transport Q occurs when the restoring timescale for temperature is about one-tenth of the time it takes a particle to flow around the gyre. Estimates for the actual heat transport carried by the subtropical gyre are 0.2–0.4 PW for the North Atlantic and 0.3–0.6 PW for the North Pacific. Finally, the model shows that when the restoring timescale is short compared to the gyre advection timescale, the heat transport is sensitive to the width of the western boundary current. Potentially this could lead coarse-resolution numerical models to underestimate meridional heat transport, but the actual restoring timescale of the ocean may be too long for this to be an important effect.

1. Introduction

Wind-driven subtropical gyres contribute to the global meridional heat flux by advecting warm water poleward and cold water equatorward. Bye and Veronis (1980) and Wang et al. (1994, henceforth WSM) explored this component of the heat flux using barotropic numerical models in which temperature was a passive tracer governed by an advection–diffusion equation. The temperature distribution was forced by a restoring term proportional to the difference between the actual temperature and a reference temperature. This restoring term represents the combined effects of radiation and thermal interaction with the atmosphere (Haney 1971). The reference temperature was a function of latitude, decreasing from equator to pole with broadly the same pattern as observed on the earth. Advection injects anomalously cold or warm water into a given latitude while the restoring term reduces the temperature anomaly.

The strength of the restoring term is controlled by γ, the decay timescale for a temperature anomaly in the absence of motion. It would be useful to understand the role γ plays in this system and generally in ocean models with similar forcing. WSM investigated the influence of γ on properties of the system such as the meridional heat transport.

In order to gain further insight into such systems, I examine an exceedingly simple model of a fluid forced by restoring to a prescribed temperature. As in WSM and Bye and Veronis, the temperature is merely a passive tracer with no dynamical significance, but I also reduce the fluid mechanics of the system to the kinematics of water flowing at piecewise-constant speed around a circuit in a channel. This circuit schematically represents the flow of water along streamlines in a numerical model as well as the flow around more complicated trajectories in the real ocean. Diffusion of temperature is ignored in this model, allowing us to describe the resulting system by an ordinary differential equation, which can be solved analytically. The similarity between results from this model and results from WSM's model, which included diffusion, indicates that lateral diffusion is not a very significant component of heat transport within the subtropical gyre. The analytical solution shows how simple and rather general arguments about the interaction of advection and Haney-like restoring lead to the results found by the more detailed analysis of WSM. Solvable differential equations are rare in fluid mechanics: while the equation solved here is highly idealized, it may be a useful tool in thinking about some aspects of the interaction of kinematics and thermodynamics in the general circulation of the ocean.

2. Temperature equation and its solution

Imagine water flowing through a channel that is connected to itself to make a closed circuit (Fig. 1). This

Corresponding author address: Dr. Barry A. Klinger, Nova Southeastern Oceanographic Center, 8000 North Ocean Drive, Dania, FL 33004.
E-mail: klinger@ocean.nova.edu

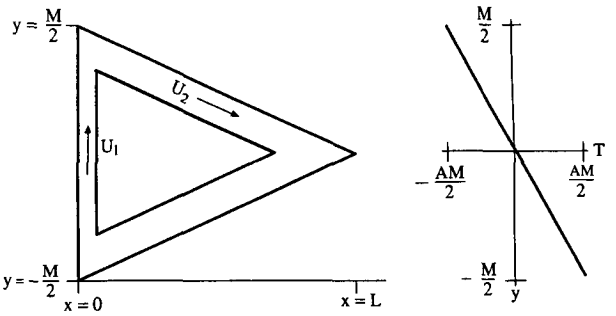

FIG. 1. Particle trajectory idealized as channel circuit. To the right of the circuit is the reference temperature profile.

arrangement represents the flow of water within a streamtube in barotropic flow such as in WSM. The triangular shape of the channel is a crude approximation of flow in the subtropical gyre, with fast northward flow in the "western boundary current" (WBC) and slow southward flow in the rest of the "gyre." The mathematical analysis below will be precisely true for other streamtube patterns as well, as long as each streamtube's zonal width, and hence its meridional velocity, is independent of latitude in the regions of southward and northward flow. Measuring arclength around the channel by s, the water temperature $T(s)$ is relaxed to a reference temperature $T_0(s)$, which is cold in the northern part of the channel loop and warm in the southern part. The temperature of the water at position s, flowing at speed $u(s)$, is then

$$u\frac{dT}{ds} = \gamma(T_0(s) - T). \tag{1}$$

To capture the difference between the WBC and the gyre, the fluid is prescribed to have a high velocity U_1 in the WBC and a low velocity U_2 in the rest of the gyre. To satisfy continuity for an incompressible fluid, the channel must be narrower in the western boundary current then in the gyre so that $w_1U_1 = w_2U_2$ for channel width w. The reference temperature is simply

$$T_0(y) = -Ay, \tag{2}$$

where y is the meridional coordinate and varies from $-M/2$ to $M/2$. Inserting (2) into (1) and using a length scale of M and temperature scale of AM to nondimensionalize the resulting equation, we obtain

$$\frac{dT}{ds} = -\frac{\gamma M}{u}(T + y). \tag{3}$$

We solve (3) separately for $T = T_1$ in the western boundary current and for $T = T_2$ in the gyre, and use the condition that $T_1 = T_2$ at the entrance and exit of the WBC to combine the solutions.

It is convenient to solve (3) in terms of $T(y)$ rather than $T(s)$. In the WBC, $dT/ds = dT/dy$, and in the gyre,

$$\frac{dT}{ds} = -\frac{dT/dy}{\sqrt{1 + (2L/M)^2}}, \tag{4}$$

where L is the zonal extent of the channel circuit (see Fig. 1). Solving (3) in each region and matching the solutions at $y = \pm 1/2$, we find that

$$T_1 = -y + \frac{1}{\omega} - \left(\frac{1}{\omega} + \frac{1}{\lambda}\right)\left(\frac{1 - e^{-\lambda}}{e^{\omega} - e^{-\lambda}}\right)e^{-\omega(y-1/2)} \tag{5a}$$

$$T_2 = -y - \frac{1}{\lambda} - \left(\frac{1}{\omega} + \frac{1}{\lambda}\right)\left(\frac{1 - e^{\omega}}{e^{\omega} - e^{-\lambda}}\right)e^{\lambda(y-1/2)}, \tag{5b}$$

where

$$\omega \equiv \frac{\gamma M}{U_1} = \frac{\tau_w}{\tau_r} \tag{6}$$

and

$$\lambda \equiv \sqrt{1 + (2L/M)^2}\,\frac{\gamma M}{U_2} = \frac{\gamma M}{V_2} = \frac{\tau_g}{\tau_r}. \tag{7}$$

Here τ_r, τ_w, and τ_g are timescales for, respectively, the restoring to a prescribed temperature, advection through the western boundary current, and advection in the rest of the gyre; V_2 is the meridional component of velocity, which is given by the Sverdrup relation. Given total annual-mean transports Φ of 40 and 65 Sv (Sv $\equiv 10^6$ m^3 s^{-1}), respectively, of the subtropical gyres of the North Atlantic and Pacific (Hellerman and Rosenstein 1983), basin widths L of 6000 and 10 000 km, and a scale thickness $H = 500$ m of the wind-driven flow, we find that $V_2 = \Phi/HL \approx 0.01$ m s^{-1} in both oceans. For $M = 4000$ km, this yields $\tau_g \approx 13$ yr. Han (1984) computed a measure of the restoring timescale, $D = Hc_p\rho/\tau_r$, for the World Ocean using air–sea exchange coefficients based on mean atmospheric conditions. Here $\rho \approx 1000$ kg m^{-3} is the density and $c_p \approx 4000$ J kg^{-1} °C^{-1} is the specific heat of seawater. He found that $D \approx 50$ W m^{-2} °C^{-1} was good to within about 15% for the entire Pacific and Atlantic subtropical gyres. Equation (7) and the expressions for D and V_2 may be combined to show that

$$\lambda = \frac{LMD}{\rho c_p \Phi}, \tag{8}$$

which for both Atlantic and Pacific yields $\lambda \approx 7.5$. It is interesting that when the variables are combined in this way, there is no explicit dependence on H. However, H enters implicitly because not all of the Sverdrup transport is necessarily affected by surface temperature forcing in the subtropical gyre so that the relevant part of Φ could easily be half the total, giving $\lambda \approx 15$. In

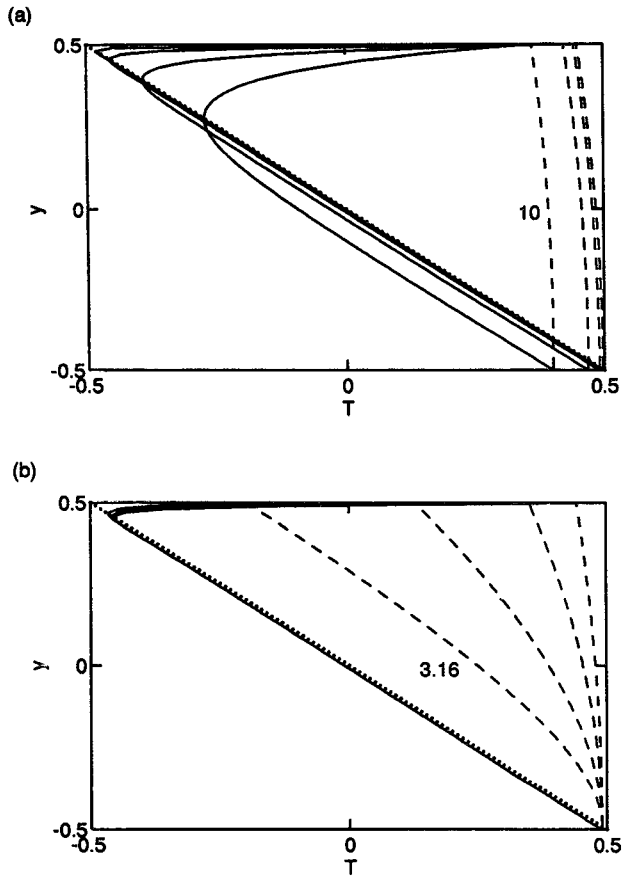

FIG. 2. Nondimensional temperature as a function of meridional distance y, for representative values of the governing nondimensional parameters, in the western boundary current (dashed line) and in the rest of the gyre (solid line). Dotted line shows reference temperature $T_0(y)$. (a) $\omega = 0.1$, $\lambda = 10, 31.6, 100, 316$ (selected value of λ marked on plot); (b) $\lambda = 100$, $\omega = 0.1, 0.316, 1, 3.16$ (selected value of ω shown on plot).

the western boundary currents, velocities are about 100 times greater than the Sverdrup interior so that ω should be around 0.1.

Figure 2 shows typical profiles of $T(y)$ in this parameter range. As we would expect, the slow-moving Sverdrupian part of the flow (T_2) is generally close to the reference temperature $T_0(y)$, while water parcels in the fast-moving western boundary current do not have time to acquire the reference temperature. When the parcel enters the Sverdrup interior, it quickly returns to the reference temperature (see Fig. 2a) in a transition layer whose width becomes narrower as λ increases [see also (5b), where the transition layer is represented by the $\exp(\lambda[y - 1/2])$ term]. The WBC also tends to be warmer for larger λ. The WBC temperature comes closer to the reference temperature as ω increases (Fig. 2b).

For very weak forcing (both ω and λ small), the temperature field becomes uniform. Note that this uniformity comes about without any diffusion to reduce temperature gradients; the field becomes smooth because a parcel of water completes several circuits of cooling and heating in the time it takes its temperature to equilibrate. In this limit, the temperature is sensitive to the size of ω and λ. When ω and λ are both big, however, their precise values do not affect the temperature very much since $T(y) \approx T_0(y)$.

The surface heat flux can be calculated from the divergence of temperature along streamlines. As Fig. 3 shows, the heat flux has the characteristic pattern observed in the North Atlantic (Isemer and Hasse 1987), with large heat fluxes in the northwest corner of the subtropical gyre. The maximum heat flux occurs where there is the greatest temperature difference between fast, northward-flowing water and the restoring temperature (Fig. 2).

The (dimensional) meridional heat flux in the channel is given by

$$Q = (AM\rho c_p H)(w_1 V_1 T_1 + W_2 V_2 T_2), \qquad (9)$$

where W_2 is the width of a zonal section in the Sverdrup part of the channel. Since by continuity $-W_2 v_2 = w_1 v_1 = w_1 U_1$, (9) is equivalent to

$$Q = (AM\rho c_p H w_1 U_1)(T_1 - T_2). \qquad (10)$$

The nondimensional heat transport $Q' = T_1 - T_2$ at the central latitude of the gyre is then given by

$$Q' = \frac{1}{\lambda}\frac{\delta + 1}{\delta}\left[1 - \frac{(1 - e^{-\lambda})e^{\delta\lambda/2} - (1 - e^{\delta\lambda})e^{-\lambda/2}}{e^{\delta\lambda} - e^{-\lambda}}\right]. \qquad (11)$$

Here we have written $\omega = \delta\lambda$, where $\delta = \tau_w/\tau_g$ is approximately equal to the ratio of the WBC width to the basin width L. It is useful to rearrange the controlling parameters this way, because now the strength of

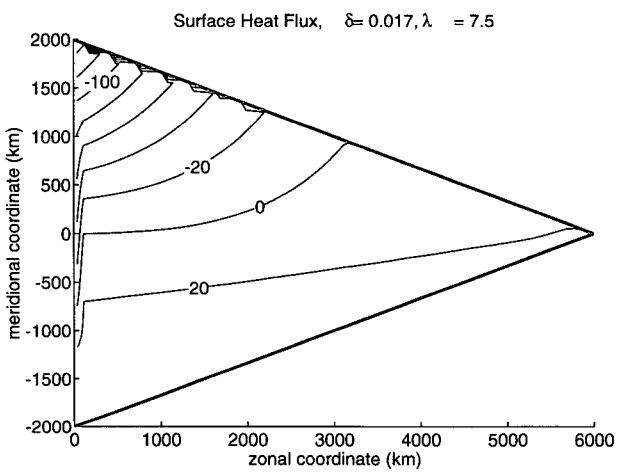

FIG. 3. Surface heat flux, for $\lambda = 7.5$, $\omega/\lambda = 0.017$, $\rho = 1000$ kg m^{-3}, $c_p = 4000$ J kg^{-1} °C^{-1}, $H = 500$ m, $L = 6 \times 10^6$ m, $V_2 = 0.01$ m s^{-1}, and $AM = 5$°C.

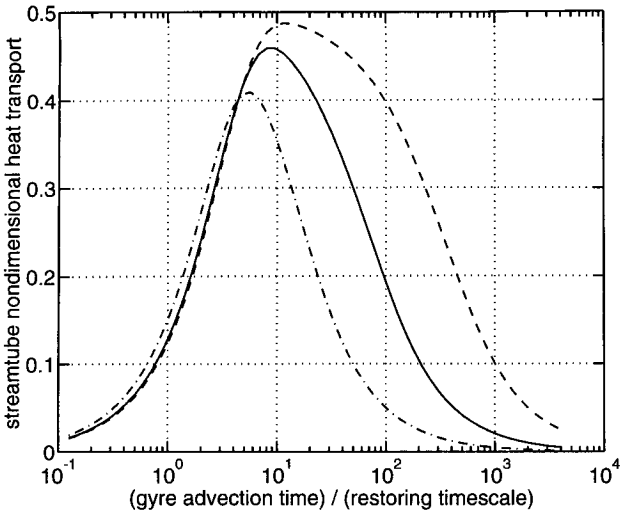

FIG. 4. Nondimensional meridional heat transport in the channel, at $y = 0$, as a function of λ for $\delta = 0.25$ (dash–dotted line), $\delta = 0.05$ (solid line), and $\delta = 0.01$ (dashed line).

the restoring constant γ is only present in one parameter, λ.

In the limits of strong and weak restoring, some algebraic manipulation shows that the asymptotes of (11) are

$$\lim_{\lambda\to\infty} Q' = (1 + 1/\delta)\frac{1}{\lambda} \qquad (12a)$$

$$\lim_{\lambda\to 0} Q' = \frac{1}{8}(\delta + 1)\lambda. \qquad (12b)$$

These expressions are consistent with similar limits found by WSM. For small δ (12a) becomes $Q' \to 1/\delta\lambda$ or $Q' \to 1/\omega$. In this limit, the temperature in the gyre is equal to the reference temperature, so the heat transport only depends on the processes in the WBC. Figure 4 shows the dependence of Q' on the full range of λ, for various widths of the WBC. Using $\delta \approx 0.05$, WSM found the peak heat transport to occur at $\lambda \approx 20$. This is quite close to the estimate based on the crude model, shown here in Fig. 4, of $\lambda = 10$. The width of the peak—about two orders of magnitude—is also similar in both the detailed calculations of WSM and the estimate shown here. Finally, (10) and (11) can be adapted to estimate the total meridional heat transport across the center of the subtropical gyre. We simply take Hw_1U_1 in (10) to represent the entire WBC flow, which must be equal to the entire Sverdrup transport; this in turn is approximately HLV_2. Using $Q' = 0.45$ and the same numerical parameters as in WSM ($\rho = 1000$ kg m^{-3}, $c_p = 4000$ J kg^{-1} °C^{-1}, $H = 500$ m, $L = 4 \times 10^6$ m, and $AM = 5$°C), we find that the peak transport (at $\lambda = 10$) is $Q \approx 0.36$ PW (1 PW = 10^{15} W). This is remarkably (and probably somewhat fortuitously) close to 0.33 PW, the peak value derived from WSM's full numerical integration.

Figure 4 also illustrates the importance of replicating the appropriate western boundary current intensity. For weak restoring ($\tau_g/\tau_r < 10$), the heat transport is approximately independent of δ. For strong restoring, the heat transport falls precipitously as the WBC becomes wider and slower. This asymmetry is apparent in (12), which shows that for large λ and moderately small δ, $Q' \propto 1/\delta$ (this formula is not appropriate when $\delta \ll 2/\lambda$). Thus, general circulation models with an unrealistically sluggish Gulf Stream could underestimate the meridional heat transport attributable to the wind-driven circulation.

We can use (10) and (11) to estimate the wind-driven heat transport in the North Atlantic and North Pacific Oceans. Using the values of AM, ρc_p, λ, and volume transport Hw_1U_1 cited above, estimates of δ and Q are given in Table 1 for a realistic western boundary current 100 km wide, and the kind of sluggish, 400-km western boundary currents often found in coarse-resolution GCMs. Assuming that all the Sverdrup transport is affected by local surface temperature forcing ($\lambda = 7.5$), the size of Q (around 0.5 PW) indicates that the subtropical gyre, especially in the Pacific, can drive a large fraction of oceanic meridional heat transport at midlatitudes. For this value of λ, the intensity of the WBC is not significant. If only half of the Sverdrup transport is involved, then a smaller, but still significant, fraction of the heat transport is driven in this way, and numerical models with sluggish western boundary currents may underestimate the heat transport by about 10%.

3. Conclusions

This note estimates the temperature field and meridional heat transport resulting from advection of warm and cold water by the horizontal wind-driven circulation. Rather than trying to solve directly for the motion,

TABLE 1. Estimates of (a) δ and (b) Q for narrow and wide western boundary currents. Heat transport Q is given in units of 10^{15} W. Values of δ are based on parameters given in text; Q is based on parameters in text and on values of δ.

Western boundary current	Atlantic		Pacific	
	(a) δ			
Narrow	0.017		0.01	
Wide	0.067		0.04	
	(b) Q			
	$\lambda = 7.5$	$\lambda = 15$	$\lambda = 7.5$	$\lambda = 15$
Narrow	0.38	0.19	0.62	0.32
Wide	0.36	0.17	0.60	0.29

I use some basic facts about the circulation, and a model of heat exchange between the atmosphere and the ocean, to derive a rough picture of the temperature field. Simple as this model is, it makes clear how the temperature field and meridional heat transport depend on the timescales for advection and temperature restoration. It provides an estimate of the temperature anomaly of the western boundary current as well as the width of the temperature boundary layer just downstream of the WBC, where the temperature approaches the restoring temperature more closely.

Like the real ocean, the model displays a large surface heat flux in the northwest corner of the domain, where warm water carried by the western boundary current (WBC) undergoes intense cooling. The model is able to reproduce the heat transport results of Wang et al. (1994), which were obtained with a numerical model: the heat transport goes to zero in the limits in which the temperature-restoring timescale τ_r is either short or long compared to the gyre-advection timescale τ_g, and the maximum heat transport occurs when $\lambda = \tau_g/\tau_r \approx 10$. The strength of the maximum heat transport is also similar to numerical estimates: 0.36 PW here as compared to 0.33 PW. In the Atlantic and Pacific Oceans, λ appears to be close to the value that makes the nondimensional heat transport Q' a maximum (for fixed δ). Estimates of dimensional values of heat transport yield 0.2 PW to 0.4 PW for the Atlantic and 0.3 PW to 0.6 PW for the Pacific. Measured total heat transport for these oceans near 24°N are 1.2 PW for the Atlantic (Hall and Bryden 1982) and 0.8 PW for the Pacific (Bryden et al. 1991). My model estimates are consistent with the notion that other processes in the Atlantic, such as thermohaline-driven flow accompanying deep-water formation, transport the bulk of the heat but that wind-driven transport is also significant. In the Pacific, where no deep water is formed, the wind-driven component plays a greater role. The model also illustrates how heat transport depends strongly on the intensity of the western boundary current for large $\lambda = \tau_g/\tau_r$. The real ocean seems to have a value of λ for which the western boundary current intensity does not greatly affect the heat transport. However, given the crudeness of the model and uncertainty in estimates of air–sea exchange coefficients, it is possible that a larger λ is appropriate for the ocean, in which case numerical model resolution would have greater influence on computed heat transport.

Acknowledgments. I conducted this research under the NOAA Atlantic Climate Change Program. J. Marotzke and X. Wang provided much useful feedback. B. Brown helped with the figures. Useful comments came from B. Cushman-Roisin, A. Tandon, and others who attended seminars on this work, as well as from the reviewers.

REFERENCES

Bryden, H. L., D. H. Roemmich, and J. A. Church, 1991: Ocean heat transport across 24°N in the Pacific. *Deep-Sea Res.*, **38,** 297–324.

Bye, J. A. T., and G. Veronis, 1980: Poleward heat flux by an ocean gyre. *Dyn. Atmos. Oceans,* **4,** 101–114.

Hall, M. M., and H. Bryden, 1982: Direct estimates and mechanisms of ocean heat transport. *Deep-Sea Res.*, **29,** 339–359.

Han, Y.-J., 1984: A numerical World Ocean general circulation model. Part II: A baroclinic experiment. *Dyn. Atmos. Oceans,* **8,** 141–172.

Haney, R. L., 1971: Surface thermal boundary condition for ocean circulation models. *J. Phys. Oceanogr.*, **1,** 241–248.

Hellerman, S., and M. Rosenstein, 1983: Normal monthly wind stress over the World Ocean with error estimates. *J. Phys. Oceanogr.*, **13,** 1093–1104.

Isemer, H. J., and L. Hasse, 1987: *The Bunker Climate Atlas of the North Atlantic Ocean.* Springer-Verlag, 218 pp.

Wang, X., P. H. Stone, and J. Marotzke, 1994: Poleward heat transport in a barotropic ocean model. *J. Phys. Oceanogr.*, **25,** 256–265.